



Conceptual studies for pressurised water reactor cores employing plutonium–erbium–zirconium oxide inert matrix fuel assemblies

A. Stanculescu^a, U. Kasemeyer^b, J.-M. Paratte^{a,*}, R. Chawla^{a,c}

^a Paul Scherrer Institute, CH-5232 Villigen PSI, Switzerland

^b Institutt for energiteknikk, OECD Halden Reactor Project, N-1751 Halden, Norway

^c Swiss Federal Institute of Technology, CH-1015, Lausanne, Switzerland

Abstract

The most efficient way to enhance plutonium consumption in light water reactors is to eliminate the production of plutonium all together. This requirement leads to fuel concepts in which the uranium is replaced by an inert matrix. At PSI, studies have focused on employing ZrO₂ as inert matrix. Adding a burnable poison to such a fuel proves to be necessary. As a result of scoping studies, Er₂O₃ was identified as the most suitable burnable poison material. The results of whole-core three-dimensional neutronics analyses indicated, for a present-day 1000 MW_e pressurised water reactor (PWR), the feasibility of an asymptotic equilibrium four-batch cycle fuelled solely with the proposed PuO₂–Er₂O₃–ZrO₂ inert matrix fuel (IMF). The present paper presents the results of more recent investigations related to ‘real-life’ situations, which call for transition configurations in which mixed IMF and UO₂ assembly loadings must be considered. To determine the influence of the introduction of IMF assemblies on the characteristics of a UO₂-fuelled core, three-dimensional full-core calculations have been performed for a present-day 1000 MW_e PWR containing up to 12 optimised IMF assemblies. © 1999 Elsevier Science B.V. All rights reserved.

1. Introduction

The inventories of spent uranium fuel, and hence of plutonium generated by the operation of commercial nuclear power plants, are continuously increasing. The strategy presently adopted by some utilities to deal with this problem consists in reprocessing the spent fuel, fabricating plutonium–uranium mixed oxide (MOX) fuel assemblies, and using these to load up to one third of the core. Both reprocessing and MOX fuel fabrication are, in the countries where utilities have opted for this strategy, well-established industrial activities. A one-third MOX core loading, however, permits one only to stabilise the plutonium mass flow since, over the life span of the core loading, as much plutonium is produced through neutron captures in ²³⁸U as is consumed. To go beyond this ‘self-generated’ mode, strategies with up to

100% MOX core loadings are presently being investigated, for which, however, certain operational and safety-related problems remain to be solved. A much more efficient way to enhance plutonium consumption in light water reactors (LWRs) would obviously be to eliminate the plutonium production all together. This requirement leads to fuel concepts in which the uranium is replaced by an inert matrix.

At PSI, studies have focused on employing ZrO₂ as an inert matrix [1]. This material is stabilised by rare earth oxides into a single-phase solid solution with a highly radiation-resistant cubic structure. From the material technological viewpoint, it thus becomes comparable to UO₂ in MOX fuel, being able to host plutonium, the higher actinides and the fission products. For reactivity control reasons, adding a burnable poison to such a fuel proves to be necessary. As a result of scoping studies addressing basic reactor physics characteristics (e.g. depletion-dependent reactivity variation, reactivity control, temperature and void coefficients), Er₂O₃ was identified as the most suitable burnable poison material

* Corresponding author. Fax.: +41-56 310 4412; e-mail: jeanmarie.paratte@psi.ch

[2,3]. The results of whole-core three-dimensional neutronics analyses [4,5] indicated that, for a present-day 1000 MW_e pressurised water reactor (PWR), a four-region core fuelled solely with the proposed PuO₂–Er₂O₃–ZrO₂ inert matrix fuel (IMF) was feasible. The main operational characteristics (e.g. cycle length and power peaking) of such a 100% IMF core were shown to be very similar to those of a conventional UO₂-fuelled loading, while the plutonium consumption capabilities (in terms of total plutonium) were shown to be approximately 2.5 times as high as in the case of 100% MOX cores [6]. When assessing these results, it must be stressed, however, that they apply mainly within the scope of the studies conducted (i.e. equilibrium cycle situations and homogeneous IMF assembly design).

This paper presents the results of more recent investigations related to ‘real-life’ situations, that call for transition configurations in which mixed IMF and UO₂ assembly loadings must be considered.

2. Scope of the study

The scope of the present study has essentially been to determine the effects of the stage-wise introduction of IMF assemblies on the core characteristics of a standard UO₂-fuelled PWR.

From past experience made with MOX fuel, it must be assumed that an eventual utilisation of IMF assemblies in present-day LWRs will be gradual. Therefore, from a practical point of view, after investigating the feasibility of asymptotic 100% IMF fuel cycles, core design efforts must be concentrated on studies dealing with mixed UO₂–IMF loadings. Given the strong spectral differences to be expected in adjacent assemblies of such loadings, these studies must focus, in the first place, on the power distribution within the IMF assembly itself, since unacceptable power peaks in the neighbourhood of the UO₂ assembly cannot be excluded a priori.¹ The result of these studies has been an IMF assembly design optimised in the context of the power distribution with a surrounding of UO₂ assemblies [5,6].

The next step has consisted in assessing the core physics characteristics of mixed configurations loaded with an increasing number of such optimised IMF assemblies.

¹ At beginning-of-life (BOL), the spectral differences at the interface of IMF and UO₂ assemblies would be expected to be even more pronounced than in the UO₂–MOX case, due to the greater thermal neutron absorption rates in the IMF as compared to MOX. The enhanced absorption cross-sections in the IMF result from (a) the presence of the burnable poison and (b) the considerably higher plutonium content of the fuel.

3. Computational methods and models

3.1. IMF assembly optimisation

The IMF assembly optimisation calculations were performed with the help of the two-dimensional transport-theory burnup code BOXER, that is part of the ELCOS code system [7]. BOXER is a modular code whose main parts are:

- *Cell calculation*: In the configuration to be treated, the most important cell from the point of view of the neutron spectrum is chosen as the ‘principal cell type’. It is calculated with white boundary conditions. Its outgoing partial currents can be used as boundary conditions for the other cell types and for homogeneous regions. The cell calculation begins with the resonance calculation in two material zones and about 8000 lethargy points depending on the composition of the resonance material. The resulting ultra-fine spectrum is used as weighting function to condense the pointwise cross-sections into groups. Afterwards, a one-dimensional flux calculation is performed in all zones of the cell, based on a transport method in cylindrical or slab geometry and in 70 energy groups. Then, the cross-sections for the cell are condensed spatially as well as energetically.
- *Two-dimensional modules*: The configuration is represented by an X – Y mesh grid. The flux distribution is calculated based on either a diffusion or a transport module. The results are the multiplication factor, k_{eff} , the neutron flux, the power distribution and the reaction rates. A spatial and energetic condensation of the group constants produces the input data for the correlation code CORCOD which computes the coefficients of the polynomials used to represent the BOXER results, thus establishing the input library for the three-dimensional nodal core simulator SILWER (see Section 3.2).
- *Burnup*: The variation of the isotopic densities in each material of the configuration is calculated using reaction rates collapsed to one group by weighting with the multigroup fluxes from the cell and the two-dimensional calculations. The time dependence of the nuclide densities is described by Taylor series. The densities of nuclides with high destruction rates are assumed to be asymptotic. An iterative correction adjusts the fluxes within the time step in order to keep the power constant. The effect of the changing spectrum on the reaction rates is taken into account by a predictor–corrector method and by density dependent one-group cross-sections within the time step for ²³⁹Pu and ²⁴⁰Pu (each approximated by a rational function). A time step can be divided into several micro-steps without recalculating the reaction rates in order to improve the numerical accuracy of the depletion calculation.

For most isotopes, the cross-section library is based on the JEF-1 file [8], notable exceptions being the Er and the ^{155}Gd cross-sections, based on BROND-2 [9] and JENDL-2 [10] data, respectively.

The model employed consisted of a 3×3 array, with the IMF assembly being located in the centre and surrounded by standard UO_2 assemblies. The plutonium considered in the IMF corresponds to reprocessed LWR-fuel having reached an average discharge burnup of about $42 \text{ GW d t}_{\text{HM}}^{-1}$ ($\sim 66 \text{ wt\%}$ fissile plutonium content [11]).

3.2. Analyses of mixed UO_2 -IMF cores

For these analyses, three-dimensional full-core calculations for a present-day 1000 MW_e PWR containing up to 12 IMF assemblies have been performed with the help of the nodal core simulator SILWER, also part of the ELCOS code system. SILWER applies an analytical nodal method to solve the two-group neutron diffusion equations.

The introduction of the optimised IMF assemblies into a UO_2 -fuelled PWR was considered in the context of a four-batch core configuration representing a ‘real-life’ loading of an actual power reactor having 177 assemblies. The reference ^{235}U enrichments were 3.8, 3.5 and 3.4 wt\% . In a first step, four fresh IMF assemblies replaced the standard UO_2 assemblies with the highest relative nodal power values. Starting with this configuration, ensuing burnup calculations permitted to establish an appropriate fuel management scheme for this mixed UO_2 -IMF core. Thus, after each cycle, while taking care that the overall one-fourth core symmetry was preserved, the IMF assemblies were shuffled to positions which would have been occupied by UO_2 assemblies with the same burnup state.

4. Results

4.1. IMF assembly optimisation

First results of the optimisation efforts showed that, for homogeneous IMF assemblies, strong power peaking (maximum peaking factor of 1.65, to be compared with 1.48 for a MOX assembly) occurred when both the IMF and the surrounding UO_2 fuel were fresh. As was to be expected, the maximum values in the IMF assembly occurred in the outermost fuel rod positions, while the effect on the power distribution inside the assembly was limited.² Accordingly, optimisation efforts,

² The larger thermal neutron absorption cross-sections in the IMF assembly, as compared to MOX (see earlier footnote), render the spectral influence of the surrounding UO_2 assemblies relatively weak for fuel rod positions well within the assembly.

considering also depletion-dependent effects, focused on the fuel rods at the edge of the IMF assembly. The result of the optimisation work is shown in Fig. 1 (quarter-assembly view). The main features of the proposed IMF assembly are the following:

- introduction of a central water hole, in order to yield a smoother burnup distribution;
- for the fuel rods at the periphery, reduction of the plutonium content by approximately 16% compared to the inside rod positions;
- for the outermost corner rod, reduction of the plutonium content by approximately 26% compared to the inside rod positions, and additional Gd poisoning (the latter was preferred over a further increase of the Er content, since the fast burning Gd isotopes permit to attain a better power distribution towards end of life);
- a slightly increased plutonium content for all the remaining inner fuel rod positions, in order to attain the same average plutonium content as in the earlier homogeneous IMF assembly design.

The burnup calculations indicated that, due to the additional positioning with Gd of the outermost corner rod of the optimised IMF assembly, the maximum power peaking would occur at the end of the first, and at the beginning of the second, cycle.

Fig. 2 shows the distribution of the relative power density for the optimised IMF assembly surrounded by eight standard UO_2 assemblies at the end of the first burnup cycle. Compared to the homogeneous non-optimised IMF assembly, the power peak is decreased by approximately 28%. The power distributions obtained are thus comparable to those of mixed UO_2 -MOX core loadings as presently realised in LWRs.

4.2. Analyses of mixed UO_2 -IMF cores

As indicated earlier, the first study currently undertaken concerns the influence on the core characteristics of introducing four of the optimised IMF assemblies

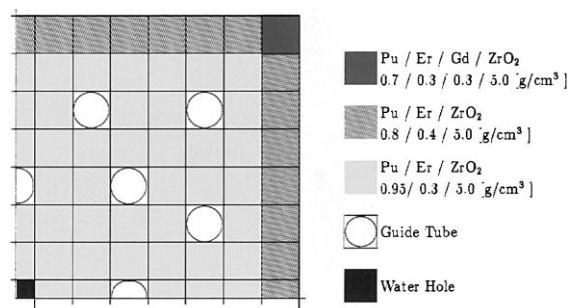


Fig. 1. Quarter-assembly view of the optimised IMF assembly for deployment in mixed UO_2 -IMF PWR core configurations.

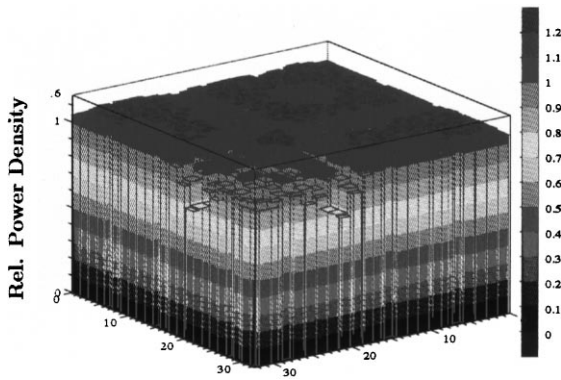


Fig. 2. Relative power density in the optimised IMF assembly (surrounded by UO₂ assemblies) at the end of the first cycle (350 effective full-power days).

into a present-day PWR. Apart from the detailed power distribution, none of the operational characteristics (soluble-boron concentration, etc.) are altered in any significant manner as compared to the standard UO₂-fuelled core. The relative nodal power densities for the beginning-of-cycle (BOC) configuration are shown in Fig. 3 (one-fourth core symmetry). As mentioned in Section 3.2, the IMF assemblies were loaded into UO₂-assembly peak power positions (i.e. B-8 and H-14, and the corresponding two other symmetrical positions). The first and second lines give the relative nodal power values for the reference UO₂-fuelled core and for the mixed UO₂-IMF loading, respectively, while the third line gives the percentage change in the nodal power densities upon introduction of the IMF assemblies into the reference UO₂ core. As seen in Fig. 3, the IMF assemblies have lower relative nodal power density (reduced by

| | 8 | 9 | 10 | 11 | 12 | 13 | 14 | 15 |
|----------|------|------|------|------|------|------|------|------|
| H | 0.79 | 1.18 | 1.24 | 1.21 | 1.43 | 0.91 | 1.5 | 0.65 |
| | 0.87 | 1.3 | 1.34 | 1.28 | 1.41 | 0.75 | 0.95 | 0.44 |
| | 11 | 10 | 8 | 6 | -1 | -17 | -37 | -32 |
| G | 1.18 | 1.2 | 1.25 | 1.16 | 1.05 | 0.88 | 1.47 | 0.9 |
| | 1.3 | 1.32 | 1.35 | 1.24 | 1.06 | 0.8 | 1.16 | 0.7 |
| | 10 | 11 | 9 | 7 | 1 | -10 | -21 | -22 |
| F | 1.24 | 1.25 | 1.1 | 1 | 0.82 | 0.83 | 1.1 | 0.41 |
| | 1.34 | 1.35 | 1.19 | 1.07 | 0.85 | 0.81 | 1.01 | 0.35 |
| | 8 | 9 | 8 | 7 | 4 | -2 | -8 | -13 |
| E | 1.21 | 1.16 | 0.99 | 0.87 | 1.44 | 1.3 | 0.53 | |
| | 1.28 | 1.24 | 1.06 | 0.93 | 1.5 | 1.36 | 0.53 | |
| | 6 | 7 | 7 | 8 | 4 | 4 | 0 | |
| D | 1.43 | 1.05 | 0.81 | 1.44 | 1.16 | 1.09 | 0.33 | |
| | 1.41 | 1.06 | 0.85 | 1.5 | 1.24 | 1.16 | 0.33 | |
| | -1 | 1 | 5 | 4 | 7 | 6 | 1 | |
| C | 0.91 | 0.88 | 0.83 | 1.3 | 1.09 | 0.41 | | |
| | 0.75 | 0.79 | 0.81 | 1.36 | 1.16 | 0.43 | | |
| | -18 | -10 | -2 | 4 | 6 | 3 | | |
| B | 1.5 | 1.48 | 1.11 | 0.53 | 0.33 | | | |
| | 0.95 | 1.16 | 1.01 | 0.53 | 0.33 | | | |
| | -37 | -21 | -9 | 0 | 1 | | | |
| A | 0.64 | 0.9 | 0.41 | | | | | |
| | 0.44 | 0.7 | 0.35 | | | | | |
| | -32 | -22 | -14 | | | | | |

UO₂
 IMF
 %-Diff.

Fig. 3. Comparison of radial nodal power distributions (one-fourth core symmetry) at beginning-of-cycle (BOC) for the reference UO₂-fuelled case (first-line) and the mixed UO₂-IMF loading (second line), the percentage difference being indicated in the third line. Position H-8 indicates the core centre, the four optimised IMF assemblies having been loaded into positions B-8, H-14 and the corresponding two symmetrical positions.

approximately 37%, as compared to the replaced UO_2 assemblies), while the increase in the values for the other UO_2 assemblies does not exceed 11%. The maximum linear rating attained in the IMF assemblies is thus approximately one-third lower than that obtained in the reference UO_2 core.

Obviously, power peaking in the IMF assemblies increases with burnup, since the burnable poison is depleted (especially Gd in the outermost corner rod position). As can be seen from Fig. 4, even at the end of the first cycle, the IMF assemblies have approximately 9% lower relative nodal power values than those which the UO_2 assemblies would have had at the same location. The maximum linear rating of the IMF assemblies increases by approximately 20% with respect to the BOC values. The relative nodal power distribution results of the three-dimensional full-core calculations are also displayed graphically in Fig. 5 for the reference UO_2

core at BOC, as well as for the mixed UO_2 –IMF core at both BOC and EOC.

The power peaking results obtained for the IMF assemblies at the end of the first cycle were not exceeded in any of the following burnup cycles for which SILWER simulations were carried out, confirming the qualitative findings of the IMF assembly optimisation study (see Section 4.1).

In a further study, a BOC configuration with eight more IMF assemblies was considered. These additional assemblies were also loaded into positions of high power density in the reference UO_2 core (at positions D-11, E-12 (see Fig. 3) and the corresponding symmetrical positions in the other three quadrants). Also for this mixed configuration with 12 IMF assemblies, the BOC operational core characteristics were very similar to those of the UO_2 reference case, with the exception of the critical soluble-boron concentration which was somewhat

| | 8 | 9 | 10 | 11 | 12 | 13 | 14 | 15 |
|----------|------|------|------|------|------|------|------|------|
| H | 0.82 | 1.11 | 1.13 | 1.13 | 1.31 | 0.93 | 1.36 | 0.71 |
| | 0.81 | 1.08 | 1.11 | 1.11 | 1.3 | 0.88 | 1.25 | 0.66 |
| | -2 | -2 | -2 | -2 | -1 | -5 | -8 | -7 |
| G | 1.11 | 1.12 | 1.16 | 1.13 | 1.06 | 0.94 | 1.34 | 0.95 |
| | 1.08 | 1.09 | 1.13 | 1.11 | 1.05 | 0.92 | 1.29 | 0.95 |
| | -2 | -3 | -2 | -2 | -1 | -2 | -4 | -1 |
| F | 1.14 | 1.16 | 1.08 | 1.02 | 0.89 | 0.9 | 1.13 | 0.52 |
| | 1.11 | 1.13 | 1.05 | 1.01 | 0.88 | 0.89 | 1.13 | 0.53 |
| | -2 | -2 | -2 | -2 | -1 | -1 | 0 | 1 |
| E | 1.13 | 1.12 | 1.02 | 0.92 | 1.33 | 1.24 | 0.65 | |
| | 1.11 | 1.1 | 1.01 | 0.9 | 1.31 | 1.23 | 0.65 | |
| | -2 | -2 | -2 | -2 | -1 | -1 | 0 | |
| D | 1.31 | 1.06 | 0.89 | 1.33 | 1.1 | 1.09 | 0.44 | |
| | 1.3 | 1.05 | 0.88 | 1.31 | 1.09 | 1.08 | 0.43 | |
| | -1 | -1 | -1 | -2 | -2 | -1 | -3 | |
| C | 0.93 | 0.93 | 0.9 | 1.24 | 1.09 | 0.53 | | |
| | 0.88 | 0.92 | 0.89 | 1.23 | 1.08 | 0.51 | | |
| | -5 | -2 | -1 | -1 | -1 | -3 | | |
| B | 1.36 | 1.34 | 1.12 | 0.65 | 0.44 | | | |
| | 1.24 | 1.29 | 1.13 | 0.65 | 0.43 | | | |
| | -9 | -4 | 1 | 0 | -3 | | | |
| A | 0.71 | 0.95 | 0.52 | | | | | |
| | 0.66 | 0.94 | 0.52 | | | | | |
| | -7 | 0 | 1 | | | | | |

| |
|---------------|
| UO_2 |
| IMF |
| %-Diff. |

Fig. 4. Comparison of radial nodal power distributions (one-fourth core symmetry) at end-of-cycle (EOC) for the core configurations for which the BOC results are given in Fig. 3.

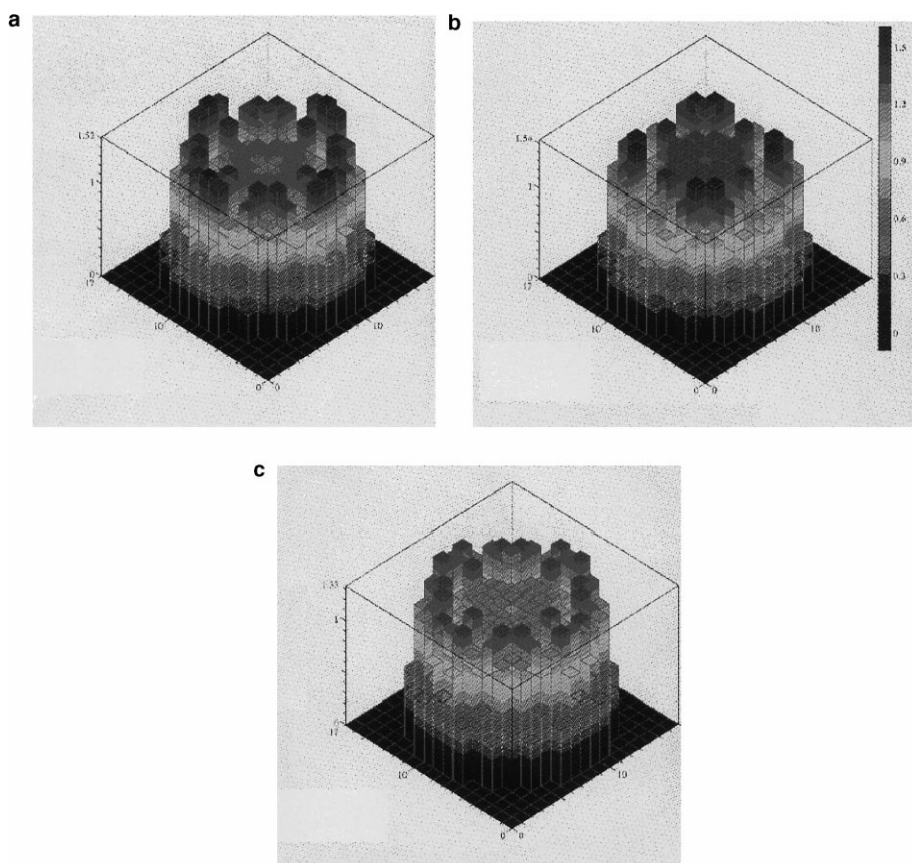


Fig. 5. Schematic views of the relative power distributions for (a) the reference UO₂-fueled PWR at BOC, and for the mixed UO₂-IMF core (containing four optimised IMF assemblies) at (b) BOC and (c) EOC.

lower. Burnup calculations showed that the power distribution throughout the first cycle remains qualitatively similar to that for the reference core, clearly indicating the feasibility of even larger IMF loadings.

4.3. Plutonium consumption

No attempts have currently been made for the definition of detailed fuel management schemes that would go beyond the 12-IMF-assembly loading considered above, i.e. towards full IMF core loadings. Thus, at this stage, an important caveat has to be made when assessing the plutonium consumption capabilities of partially loaded IMF cores. Effectively, caution is due when assessing absolute plutonium consumption rates, since the only basis available in this context is that provided by the studies performed for 100% uranium-free PWR loadings fuelled with homogeneous IMF assemblies [4]. However, conclusions regarding the relative plutonium consumption potential of IMF-loaded PWRs, as compared to MOX-fuelled cores, can be easily drawn based on the results of the earlier

conducted studies on full core loadings of IMF and MOX. The results reported in [4,5] indicate that the plutonium (reactor-grade) consumption rates for 100% MOX and 100% uranium-free (IMF) PWR cores are about 430 and 1090 kg GW_e⁻¹ a⁻¹, respectively. This means that LWRs with as little as about one-eighth (i.e. 24 assemblies in the present-day 1000 MW_e PWR considered in this study) IMF core loadings would operate in the 'self-generated' mode (as compared to one-third MOX-fuelled cores).

5. Conclusions

The results currently presented strengthen the case for a gradual introduction of uranium-free IMF assemblies into a present-day 1000 MW_e PWR. It has been shown that loading up to 12 IMF assemblies, having the optimised design proposed in this paper, can be done with fuel management schemes that are quite compatible with current operational requirements (i.e. cycle length, soluble-boron concentration, etc.). Clearly, additional

studies are necessary to define a detailed fuel management strategy going beyond the 4–12 IMF assemblies considered presently, i.e. towards 100% IMF loadings. Nevertheless, relative plutonium consumption rates can be easily derived from the earlier reported studies on 100% IMF and MOX cores. These indicate a plutonium reduction potential approximately 2.5 times higher in the IMF case as compared to MOX, thus underlining the considerable economic incentive for PWR cores with partial loadings of IMF assemblies.

References

- [1] C. Degueldre, U. Kasemeyer, F. Botta, G. Ledergerber, *Mater. Res. Soc. Symp. Proc.* 412 (1995) 15.
- [2] J.-M. Paratte, R. Chawla, *Ann. Nucl. Energy* 22 (1995) 471.
- [3] U. Kasemeyer, J.-M. Paratte, R. Chawla, Reactor physics characteristics of possible fuel materials for plutonium-incinerating LWRs, in: *Proc. IAEA Technical Committee Meeting on Unconventional Options for Plutonium Disposition*, Obninsk, Russia, Nov. 7–11, 1994.
- [4] U. Kasemeyer, P. Grimm, J.-M. Paratte, R. Chawla, *Nucl. Technol.* 121 (1998) 52–63.
- [5] U. Kasemeyer, PhD thesis No. 1757, Swiss Federal Institute of Technology, Lausanne, 1998.
- [6] G. Ledergerber, C. Degueldre, U. Kasemeyer, A. Stanculescu, J.-M. Paratte, R. Chawla, Using civilian plutonium in LWRs with an inert matrix fuel, in: *Proceedings of the International Conference on Future Nuclear Systems (GLOBAL '97)*, vol. 2, 1997, p. 1068.
- [7] J.-M. Paratte, K. Foskolos, P. Grimm, C. Maeder, Das PSI-Codesystem ELCOS zur stationären Berechnung von Leichtwasserreaktoren, in: *Proceedings of Jahrestagung Kerntechnik*, Travemünde, Germany, 17–19 May, 1988.
- [8] J. Rowlands, N. Tubbs, The joint evaluated file, a new data resource for reactor calculations, in: *Proceedings of the International Conference on Nuclear Data for Basic and Applied Science*, Santa Fe, New Mexico, 13–17 May, 1985.
- [9] A.I. Blokhin et al., Current status of Russian evaluated neutron data libraries (Files BROND-2, FOND and ABBN-90), in: *Proceedings of the International Conference on Nuclear Data for Science and Technology*, Gatlinburg, Tennessee, 9–13 May, 1994, American Nuclear Society, vol. 2, 1994, p. 695.
- [10] Y. Kikuchi, Present status and benchmark tests of JENDL-2, in: *Proceedings of the International Conference Nuclear Data for Science and Technology*, Antwerp, Belgium, 6–10 Sept. 1982.
- [11] J. Bouchard, Influence des stratégies du cycle du combustible sur le choix des réacteurs de nouvelle génération, in: *Proceedings of the International ENS Topical Meeting on Next Generation LWRs (TOPNEX '93)*, The Hague, The Netherlands, 1993.